SiCN Amorphous Materials Chemical Vapour Deposited Using the Si(CH3)4-NH3-H2 System

A. Bendeddouche, R. Berjoan, E. Bêche, Sylvie Schamm-Chardon, V. Serin, Robert Carles, R. Hillel

JOURNAL DE PHYSIQUE IV
Colloque C5, supplément au Journal de Physique II, Volume 5, juin 1995

SiCN Amorphous Materials Chemical Vapour Deposited Using the $Si(CH_3)_4$-NH_3-H_2 System

A. Bendeddouche, R. Berjoan*, E. Bêche**, S. Schamm***, V. Serin***, R. Carles**** and R. Hillel

IMP-CNRS, University of Perpignan, 66860 Perpignan cedex, France
** IMP-CNRS, BP. 5, Odeillo, 66120 Font-Romeu, France*
*** LERMPS.IPSé, 90010 Belfort cedex, France*
**** CEMES-LOE/CNRS, BP. 4347, 31055 Toulouse cedex, France*
***** URA 74 du CNRS, University of Toulouse III, 31062 Toulouse cedex, France*

Abstract. Elaboration of amorphous SiCN materials was performed using a conventional thermaly activated CVD at 1000-1200°C from the TMS-NH_3-H_2 system. The influence on the deposition rate and the composition was investigated using an experimental design by varying: deposition temperature, pressure and NH_3 flow rate. A set of 16 samples SiC_xN_y with x/y ranged from 0.04 to 1.69 was prepared. Accurate determination of the elemental compositon required EPMA-WDS and XPS and occasionally RBS analyses. The chemical bonding system was investigated by XPS and Raman spectroscopy. Comparisons between CVD prepared silicon carbide and nitride reference samples and the SiC_xN_y materials were achieved. It was concluded that for $x/y < 0.15$, Si-N was predominant, whereas for $x/y \geq 0.86$, the amorphous deposits mainly contain Si-N and Si-C, and additionally carbon bonds including C-Si and C-C, and probably a rather low C-N contribution. Raman study shown that C-C bonding could be related to a carbon excess acting as a binder in-between the tetrahedral networks of Si-C and Si-N. The first results of EXELFS concerning a carbon poor deposit shown that Si has a first coordination shell similar to that of Si_3N_4.

1. INTRODUCTION

Si_3N_4 and SiC exhibit several interesting properties. For instance, the good strength and thermal-shock behaviour of the nitride is well known, whereas the carbide has a higher thermal conductivity, a better hardness, creep and oxidation resistance [1-2]. Additionally, Si_3N_4 is an electric insulator whereas SiC is a semiconductor. Hence, the challenge is to combine these complementary characteristics in a same material. Amorphous mixtures of Si_3N_4-C were chemical vapour codeposited using $SiCl_4$-NH_3-C_3H_8-H_2 [3]. Amorphous SiCN:H films were produced either by metal organic CVD using organosilazanes as single source [4-5], or by plasma-enhanced CVD from hexamethyldisilazane and nitrogen [6] or usingSiH_4-NH_3-CH_4 (or C_2H_4)-H_2 [7-8]. With the last precursors in the range 220-500°C, it was reported a continuous evolution of composition and bonding structure of SiC_xN_y:H films between SiC_x:H and SiN_y:H [9]. At 600°C by plasma-activated CVD from $Si(CH_3)_4$-NH_3-Ar, amorphous SiCN coatings with continuous composition between Si_3N_4 and SiC were obtained. The chemical environments of the Si, C and N atoms were considered as more complicated as in a mixture of the pure phases [10]. From the same precursors and with hydrogen instead of argon, amorphous SiC_xN_y films were prepared by low pressure CVD at 1200°C. From the optical gap measurements versus film composition, it was suggested that these materials could be an alloy phase [11].

Using a CVD process, we aimed to prepare SiCN amorphous coatings of controlled composition and thickness. For this purpose, the handly gas source system $Si(CH3)_4$-NH_3-H_2 was chosen. In those amorphous materials Si-C and Si-N chemical bondings are expected to exist either separated in two phases or/and combined in one phase. Moreover, because of the nanometric size of the phases, the resulting materials could get improved and/or new properties [12]. Since the chemical and structural organization extend very small scale in such compounds, their characterization required cross-checking of different data from complementary techniques. For this purpose, electron probe microanalysis-wavelength-dispersive spectrometry (EPMA-WDS), X-ray photoelectron spectroscopy (XPS) and Rutherford backscattrering

spectrometry (RBS) were used to determine the elemental compositions. Characterization of the chemical bonding system in the SiCN materials was provided by XPS and Raman spectroscopy. In addition, the first results of an Electron Energy Loss Spectroscopy (EELS) study, particularly EXtended Energy Loss Fine Structure (EXELFS) are presented. Its purpose is to compare the local short range order around the silicon within the SiC_xN_y deposits, in connection with their elaboration conditions and their physico-chemical properties.

2.EXPERIMENTAL PROCEDURE

2.1 Experimental device

Deposits were prepared by conventional thermal CVD under reduced pressure, in a vertical reactor chamber (silica tube: ϕ = 6.2 cm, L= 20 cm). The codeposition was realized on Joule heated graphite substrate (Le Carbone-Lorraine 1116 T; thickness= 1.2 mm; thermal expansion coefficient = 6.10^{-6} $°C^{-1}$). Its shape was designed to obtain a uniformly heated zone of 25x5 mm^2. Temperature was measured with a thermocouple (TKI). Reactant sources were TMS: $Si(CH_3)4$ vapours and gaseous NH3 in hydrogen. TMS input concentration was directly flow meter controlled provided the pressure was under 1 bar. Samples of different chemical compositions were prepared by varying both the deposition temperature (T), the experimental pressure (P) and the flow rates of the input gas species (D_{TMS}, D_{NH3} and D_{H2}). The process time: 2 hours was chosen in order to obtain a thickness deposit of at least 30 μm.

2.2 Elemental composition

Since, the analysis concerned light elements: C, N and O, besides Si, results obtained from different techniques: EPMA-WDS, XPS and RBS, were compared to determine the elemental composition of the deposits. Chromium metallized cross-sections were analysed by EPMA-WDS : CAMEBAX equipped with ODPb and TAP wavelength dispersive spectrometers; i = 40 nA, V = 15 kV; standards: Si, TiC, a CVD $SiN_{1.22}$ and Fe_2O_3. XPS measurements were performed using a CAMECA - RIBER SIA 200 electron spectrometer equipped with a MAC-2 double stage cylindrical analyzer. The excitation source was AlKα radiation (1486.6 eV). Photoelectron spectra were taken at a constant energy resolution of 1 eV. The polished surfaces were analyzed as-deposited or after sputtering for 20mn by 4 keV Ar^+ ions to remove surface contaminants. The elemental composition of some samples was also obtained from RBS of 2-MeV $^4He^+$ particles. To count the scattered particles in the laboratory coordinates direction θL=160°, a surface barrier detector was used, the resolution of which (13.5 keV) has been determined with ^{241}Am. The trace of the incident beam was 2mm^2.
The compositions were expressed with the formulation SiC_xN_y. From the estimated precisions of the data taking into account the methods of analyzis and the nature, x and y were given with ±0.06x and ±0.08y accuracies. The average amount of oxygen was: 3 ± 1 atom.%.

3. EXPERIMENTAL DESIGN

Preliminary experiments were carried out with the initial conditions: P = 0.7 bar, D_{TMS} = 0.09, D_{NH3} = 1, D_{H2} =.30 (in l/h) and temperature ranged from 1000 to 1200°C. D_{TMS} = 0.09 l/h was the minimum flow rate allowed by the device which avoided homogeneous nucleation (formation of white smokes) in the reactor. In these conditions, homogeneous, adherent and dense amorphous materials were obtained. Moreover, growth rate deposit was observed to go through a minimum at T = 1090°C. Estimates of the equilibrium compositions of the system: graphite substrate + TMS-NH_3-H_2 at the initial experimental conditions, were calculated by minimizing the Gibbs energy of the system under mass balance constraints (GEMINI II chemical equilibrium computer code + Thermodata bank). Mixtures of Si_3N_4 or SiC with very large amount of carbon were found in complete disagreement with the experimental results. The reason was certainly, because free energies of crystalline line compounds were used in these calculations, instead of values for amorphous phases, not yet known. Owing to the lack of thermodynamical prediction and with the objective to control growth rate and elemental composition of the deposited materials, the influence of three factors: temperature (T), pressure (P), and NH_3 flow rate (D) was examined using the experimental design methodology [13-14]. Because of the quadratic evolution of the growth rate versus the temperature, a second order composite design was employed. The variation ranges of the selected factors X were defined by the high: X_+, low: X_- and centre: X_0 levels of the experimental design with the corresponding coded levels X_n, so that : $X_n = (X-X_0)/(X_+-X_0)$ (table I)

Table I: The variation ranges of the experimental factors and the corresponding coded levels

experimental factor	high level		centre level		low level	
	X_+	X_n	X_0	X_n	X_-	X_n
temperature: T (°C)	1200	+1	1100	0	1000	-1
pressure: P (bar)	0.7	+1	0.55	0	0.4	-1
NH_3 flow rate: D l/h	1	+1	0.55	0	0.1	-1

This design was composed in a 2^3 factorial group of experiments with a "star" design consisting of 6 axial points and 2 centre points [14]. The design matrix with the coded levels and the measured responses (thickness and elemental composition given as SiC_XN_y) are summarised in table II

Table II: the design matrix with the coded levels of the experimental factors and the measured responses (These 16 experiments were randomly performed following the order: 1, 3, 13, 9, 2, 4, 6, 8, 10, 7, 11, 15, 16, 12, 14, and 5.)

n°	T_n	P_n	D_n	e (μm)	C_X	N_y	x/y
1	-1	-1	-1	110	0.59	0.35	1.69
2	+1	-1	-1	100	0.48	0.48	1.00
3	-1	+1	-1	37	0.44	0.51	0.86
4	+1	+1	-1	45	0.56	0.5	1.12
5	-1	-1	+1	137	0.10	1.03	0.10
6	+1	-1	+1	140	0.15	0.99	0.15
7	-1	+1	+1	85	0.17	1.05	0.16
8	+1	+1	+1	125	0.11	1.04	0.11
9	-1	0	0	90	0.32	0.76	0.42
10	+1	0	0	95	0.15	0.95	0.16
11	0	-1	0	100	0.10	1.09	0.09
12	0	+1	0	50	0.04	1.13	0.04
13	0	0	-1	40	0.55	0.45	1.22
14	0	0	+1	90	0.04	1.11	0.04
15	0	0	0	70	0.07	1.12	0.06
16	0	0	0	65	0.09	1.07	0.08

The following polynomial expressions were determined to represent the variations of the deposition thickness and the elemental composition:

$e = 66.95 + 7.97\ T_n - 42.44\ P_n + 42.44\ D_n + 72.41\ T_n^2 + 19.91\ P_n^2 + 20.62\ T_nP_n + 16.87\ T_nD_n + 22.87\ P_nD_n$

$x = 0.1117 - 0.0294\ T_n - 0.0173\ P_n - 0.3551\ D_n + 0.3222\ T_n^2 - 0.1728\ P_n^2 + 0.5022\ D_n^2$

$y = 1.043 + 0.045\ T_n + 0.050\ P_n + 0.507\ D_n - 0.486\ T_n^2 + 0.279\ P_n^2 - 0.711\ D_n^2$

In the case of the thickness, i.e the deposition rate, the three factors have significant influence. The response surfaces drawn in fig.1 shows that thickness goes through a marked minimum essentially at fixed pressure or NH_3 flow rate, the temperature varying from 1000 to 1200°C.

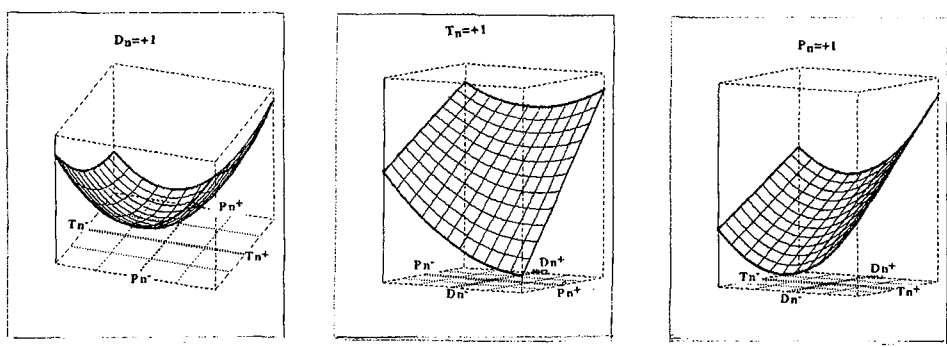

Figure 1:Response surfaces of the deposit thickness plotted as a function of T_n and P_n (D_n=+1); T_n and D_n (P_n=+1); P_n and D_n (T_n=+1)

Concerning the elemental composition expressed by SiC_xN_y, it was concluded from the examination of all the response surfaces that the effects of D_{NH3} and T were the most significant. The precise comparison of these two factors shows (fig.2) that at fixed pressure, NH_3 flow rate has a more pronounced influence than temperature. Moreover, when D_{NH3} is varied from 0.1 to 1 l/h, the amount of nitrogen in the deposit goes through a maximum while the amount of carbon goes through a minimum

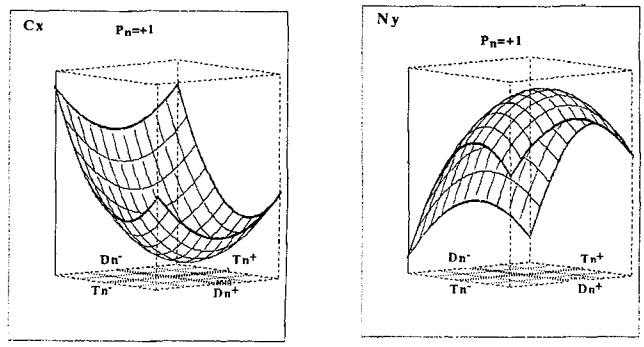

Figure 2: Response surfaces of the deposit composition (x and y) plotted as a function of T_n and D_n (P_n=+1).

4.MICROSTRUCTURAL CHARACTERIZATION

Characterization of the chemical bonding system in the SiCN materials was provided by XPS and Raman spectroscopy. In addition, EXELFS allowed to define the local arrangement around silicon. These studies needed comparisons with CVD prepared silicon carbide and nitride reference samples. A crystalline $SiC_{1.18}$ coating (TMS+H2 at 1200°C), a crystalline αSi_3N_4 deposit (TMS+NH_3+H_2 at 1300°C) and an amorphous $SiN_{1.2}$ film ($SiCl_4$+NH_3 at 1200°C) were considered for this purpose.

4.1 XPS

At first, XPS spectra were collected on the polished SiC_xN_y surfaces after sputtering for 20 minutes with 4 keV Ar+ ions. Because of charge shifting problems, it was critical to identify the chemical bonds from the experimental peak positions. This difficulty was overcame for the bonds involving silicon, by measuring the modified Auger parameter α' [15]. The measured values for the $SiC_{1.18}$ and the $SiN_{1.2}$ were 1715.3 ± 0.2 eV and 1714.0±0.2 eV respectively. For the N rich SiC_xN_y samples ($y \geq 1$), the measured α' values were found in the range 1713.5 - 1714.2 (± 0.2 eV), close to the value for Si-N bonds. For the deposits containing less nitrogen ($y \ll 1$), α' values were in the range: 1714.4 - 1715.1 (±0.2eV) in-between the Si-C and Si-N signatures.
In order to ascertain the nature of Si and C bondings in the case of $y \ll 1$, spectra were recorded from polished SiC_xN_y surfaces before and after ion bombardment. We will discuss the example of the spectra given by the $SiC_{0.32}N_{0.76}$ deposit (sample no.9 in table II).
The correponding Si 2p and C 1s lines were deconvoluted and compared with the same ones corresponding to $SiC_{1.18}$ (figure 3). The peak positions were normalized with respect to the carbon C1s line usually observed at 285 eV for adventitious carbon [15] and at 282.5eV for SiC [16]. On one hand, the C1s peaks of the two compounds recorded without ion bombardment have been fitted into four components. The peak located at 282.5 eV has been attributed to carbon bonded with silicon (C-Si) [16]. The other components are certainly the result of surface carbon contamination, i.e C-C at 284, $C_xH_yO_z$ or $Si_4C_4O_4$ at 285.3, and C-O at 287 eV [16]. On the other hand, the C1s peak of the sputtered $SiC_{1.18}$, was fitted into four components. The component at 282.5 eV indicates the presence of C-Si. The 283.9 eV one attributed to C-C bondings, results certainly from the presence of carbon excess in $SiC_{1.18}$ and also probably from the modification of the surface produced by the ionic bombardment. The two smaller peaks at 285.3 and 287 eV can be attributed to $Si_4C_4O_4$ and/or $C_xH_yO_z$ and C-O respectively. For the sputtered $SiC_{0.32}N_{0.76}$ deposit, the C1s line has been deconvoluted into four components: the two more important at 282.5 = C-Si and at 284= C-C, a small component at 286.9 = C-O and a last one at 285.2 eV. This component extracted from the broadening of the high energy side of the C1s peak is too large to be only attributed to $C_xH_yO_z$ or $Si_4C_4O_4$ as it was observed for $SiC_{1.18}$. It could be related to the presence of C-N bonds [17]. In the case of the non sputtered $SiC_{0.32}N_{0.76}$ deposit, fig 3 shows a broadening of the Si2p peak in comparison with the $SiC_{1.18}$ reference sample. Two components at 101.8 and 100.7 eV were extracted and attributed to Si-N (101.8 [18]) and Si-C (100.7 [19]). The component at 103eV related to Si-

O surface bond [20], disappears after ion bombardment. For the sputtered deposit, the component at 99.3 could correspond to Si-Si [20], which probably results from suface damage induced by ion sputtering. Analogous results were obtained from spectra recorded with other carbon rich codeposits (samples no.2 and 4 in table II). Finally, it may be concluded that the amorphous SiC_xN_y deposits with x/y ≥0.86 (y≤1) mainly contain Si-N and Si-C bonds similar to those observed in $SiC_{1.18}$ and $SiN_{1.2}$ and additionaly carbon bonds including C-Si, C-C bonds and probably a rather low C-N contribution.

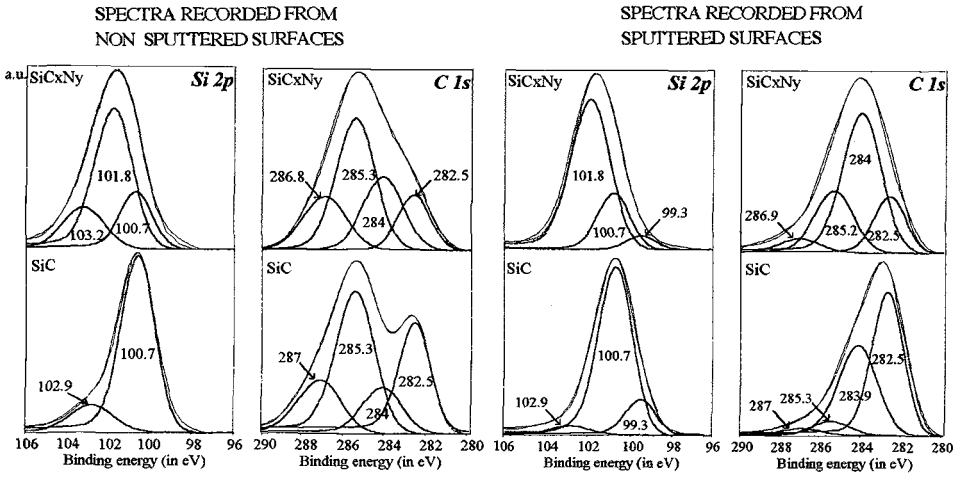

Figure 3: C1s ans Si2p XPS lines for non sputtered surfaces and ssputtered surfaces of the $SiC_{1.18}$ sample and the $SiC_{0.32}N_{0.76}$ deposit

4.2 Raman spectroscopy

The Raman spectrometer was a Dilor: 457.9 nm line of an Ar^+ laser; spectral resolution: 5.7 cm^{-1}. Spectra were recorded in backscattering geometry on the cross-section of codeposits; area of the spot beam was about $1\mu m^2$.

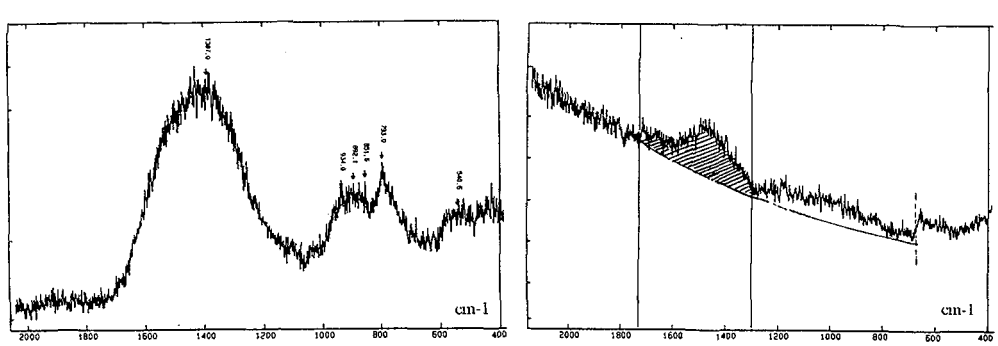

Figure 4: Raman spectra of SiC1.18 and a SiCN sample

The Raman spectrum of the $SiC_{1.18}$ (fig.4) exhibited two broad bands in the ranges 700-900 and 1200-1600 cm^{-1} that can be assigned to Si-C and C-C optical-like modes respectively. The Si-C band is divided in two sub-bands which mirror the density of states of the optical phonons in crystalline SiC [21]. This gives proof of the presence of a polycristalline SiC phase. Therefore, the C-C band, whose maximum is located around 1420 cm^{-1}, results from vibrations within the carbon excess. Although this frequency is in-between the two characteristic frequencies of a nanocrystallized graphitic carbon (1350 and 1580 cm^{-1}),

the band has not the typical "camel back" shape known for such a sp^2 C arrangement [22]. Moreover, the frequency is higher than the diamond one (C sp^3) whether it is crystallized or rather amorphous (1332 [22] and 1100-1200 cm^{-1} [23], respectively). For these reasons, the C-C band can be assigned to a disturbed sp^2 hybridization of the C atoms generated by local re-arrangements. The C atoms could be engaged in-between the SiC crystals as a binding phase with the sp^2 hybridization within the phase and "sp^2/sp^3" hybridization at the interfaces between the C phase and the SiC crystals. As a matter of fact, it has been shown that the upper C-C frequency downshifts in disordered carbon versus the disorder amount [23].
For deposits corresponding to $x/y < 0.86$, the Raman spectra were not exploitable because of very low ratio signal over background noise. Whereas, the spectra of the SiCxNy deposits with $x/y \geq 0.86$ (samples no.1 to 4 and 13 in table I) exhibited two broad bands which can be assigned to Si-C+Si-N and C-C optical-like modes situated at 700-900 [21]+800-1300 [24] and 1300-1700 cm^{-1}, respectively. The Si-C+Si-N band having no particular features, is characteristic of a highly disordered system. The C-C band being similar to that in the $SiC_{1.18}$ sample, the corresponding carbon probably presents a disturbed sp^2 hybridization. Therefore, with the SiCN deposits having an excess of carbon like in the $SiC_{1.18}$ sample, this excess carbon could act as a binder in-between the tetrahedral networks of Si-C and Si-N bonds.

4.3 EXELFS

Recent progress in Electron Energy Loss Spectroscopy (EELS) experiments allow to obtain spectra from thin films (size of analysed area on the sample of few tens nanometers) with enough signal to make EXtended Energy Loss Fine Structure (EXELFS) treatment possible [25]. The EXELFS signal appears as an oscillatory structure superimposed on the high-energy-loss side of an ionisation edge in electron energy loss spectra. Such modulations can extend up to several hundreds eV past the edge and may have a magnitude of 10 % of the signal. They result, as in EXAFS in X-ray absorption, from the interference between the outgoing excited inner-shell electron waves and the electron waves backscattered by the neighbouring atoms. The mathematical treatment, already developed for EXAFS, can be applied to EXELFS in the same way. It affords accurate information on the interatomic distances - the radial distribution function (RDF) - particularly in the case of low-Z species.

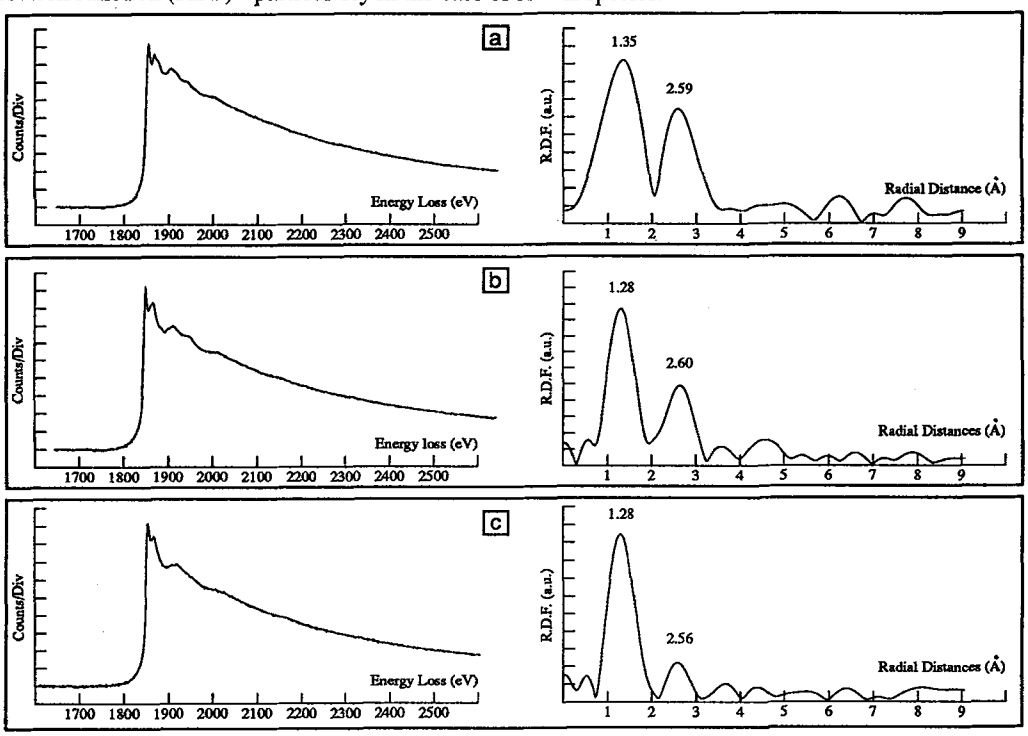

Figure 5: Si excitation K-edges (left) and associated RDF (right) for the a) $SiC_{1.18}$ reference sample b) Si_3N_4 reference sample c) the $SiC_{0.11}N_{1.09}$ deposit

The first results of an EXELFS study will be presented. This analysis concerns the Si K-edge, which appears in the spectra at 1839 eV. The C-K and N-K edges, at 284 and 401 eV respectively, could not be studied. In these cases, the extent of the oscillations beyond the edges is too limited (less than 100 eV) because of the proximity of the C-K and N-K edges in the first case and of the N-K and O-K (532 eV) edges in the second case. The purpose of this study is to compare the local short range order around the silicon within the SiC_xN_y deposits, in connection with their elaboration conditions and their physico-chemical properties.

At first, three samples were analyzed. A deposit corresponding to the average composition $SiC_{0.11}N_{1.09}$ and the two reference samples: $SiC_{1.18}$ and αSi_3N_4. Thin enough cross-sectional specimens have been prepared. TEM studies have been performed with a Philips CM30ST microscope equipped with a Gatan 666 spectrometer, with a 2 eV energy resolution. The EXELFS signals were typically recorded in an energy window ranging from 200 to 400 eV above the edge. In these experiments the probe size of the electron beam on the sample was about 60 nm and the thickness of the sample smaller than 20 nm. Radial distribution functions (RDF) have been extracted by following the original EXAFS procedure for analysis of the as-observed EXELFS signal.

At the microscopic scale, the morphology and the structure throughout the films (bright field imaging and electron diffraction) are uniform.

Typical Si - K ionization edges and corresponding RDFs functions of each sample are shown in figure 5 . The fine structures beyond the edge are rather different in the three cases. For the two reference samples they are more complex than the rather smooth ones of the SiCN sample. This corresponds to references samples crystallized at the micrometric scale, while the SiCN sample is organized only at the nanometric scale. The parameters of the EXELFS treatments are the same for the three distributions: Fourier Transform k^2 weighted taken from 30 to 290 eV (3 to 9 $Å^{-1}$), the origin of the energies being 1839 eV. When comparing the theoretical coordination shell systems around the Si atom in the SiC and Si_3N_4 structures, the only noticeable difference between the two systems is the first coordination shell. For this reason, only the first peak of the RDF functions will be discussed. The experimental distances deduced from the RDFs are listed in table III.

Table III: Comparison between the Si-C and Si-N distances deduced from the RDFs and the crystallographic values

First shell around Si		RDFmeasured value (Å) (1)	Theoretical phase shift (Å) (2) [26]	Experimental value (Å) (1) + (2)	Crystallographic value (Å)
$SiC_{1.18}$	(Si-C)	1.35	0.49	1.84	1.88
Si_3N_4	(Si-N)	1.28	0.50	1.78	1.75*
SiCN	(Si-C and/or Si-N)	1.28	-	-	-

* average value [27]

From these results, it appears that Si in the $SiC_{0.11}N_{1.09}$ sample has a first coordination shell similar to that of Si_3N_4.

5. CONCLUSION

Elaboration of amorphous SiCN materials was performed using a conventional thermaly activated CVD at 1000-1200°C from the TMS-NH_3-H_2 system. The influence on the deposition rate and the composition was investigated using an experimental design by varying three factors: deposition temperature, pressure and NH_3 flow rate. A set of 16 samples SiC_xN_y with x/y ranged from 0.04 to 1.69 was prepared. Accurate determination of the elemental compositon required EPMA-WDS and XPS and occasionally RBS analyses. The chemical bonding system was investigated by XPS and Raman spectroscopy. Comparisons between CVD prepared silicon carbide and nitride reference samples and the SiC_xN_y materials were achieved. It was concluded that for $x/y < 0.15$, Si-N was predominant, whereas for $x/y \geq 0.86$, the amorphous deposits mainly contain Si-N and Si-C, and additionally carbon bonds including C-Si and C-C, and probably a rather low C-N contribution. Raman study shown that C-C bonding could be related to a carbon excess acting as a binder in-between the tetrahedral networks of Si-C and Si-N. This interpretation is in coherency with measures of hardness and stiffness subsequently published. As a matter of fact, we will show that these mechanical characteristics are improving with the increase of the x/y ratio. Although, there are not enough proofs to ascribe the amorphous SiCN deposits as an alloy phase, it is clear that Si-N, Si-C, and C-C are strongly imbricated. The first results of EXELFS concerning a carbon poor deposit shown that Si has a first coordination shell similar to that of Si_3N_4. Other EXELFS characterizations

concerning SiC_xN_y materials with $x/y > 1$ make in progress with the purpose to study the effect of carbon enrichment on the local short range order around the silicon.

.

References

[1] Riedel R., Stercker K., and Petzow G., J. Am. Ceram. Soc. 72 (1989) 2071-2077
[2] Lange F.F., J. Am. Ceram. Soc. 56 (1973) 445-450
[3] Hirai T., and Goto T., J. Mater. Sci. 16 (1981) 17-23
[4] Maury F., Hatim Z., Reynes A., and Morancho R., Proc. of the X Intern. Conf. on CVD (Honolulu USA, Cullen G.W., and Blocher J.M. (Eds), 1987 pp.1080-1088
[5] Maury F., Hatim Z., Biran C., Birot C., Dunogues J., and Morancho R., Proc. of the VI Euro. Conf. on CVD, (Jerusalem Israel, Porat R.-Ed), 1987 pp. 390-397
[6] Gerstenberg K.W., and Beyer W., J. Appl. Phys.62 (1987) 1782-1787
[7] Kamata K., Maeda Y., and Moriyama M., J. Mater. Sci. Lett. 5 (1986) 1051-1054
[8] Moriyama M., Kamata K., and Tanabe I., J. Mater. Sci. 26 (1991) 1287-1294
[9] Zhang W., Zhang K., and Wang B., Mater. Sci. Ing. B, 26 (1994) 133-140
[10] Ducarroir M., Zhang W., and Berjoan R., J. Phys IV. 3 (1993) 247-254
[11] Ducarroir M., and Lartigue J.F., C.R. Acad. Sci. 307 (1988) 541-544 .
[12] Dagani R., Chem. and Eng. News 23 (1992) 18-24
[13] Box G.E.P., Hunter W. G., and Hunter J.S., Statistics for experimenters (John Wiley and Sons, New York, 1978)
[14] Phan Tan Luu R., Feneuille D., and Mathieu D., Méthodologie de la recherche expérimentale, (IPSOI, University of Marseille France)
[15] Briggs D., and Seah M.P., Surface analysis by Auger and X-ray photoelectron spectroscopy (Whiley, Chichester 1983)
[16] Hornetz B., Michel H.J., and Halbritter J., J. Mater. Res. 9 (1994) 3088-3094
[17] Komatsu S., Hirohata Y., Fukuda S., Hino T., and Yamashina T., Thin Sol. Films 193/194 (1990) 917-923
[18] Taylor J.A., Appl. Surf. Sc. 7 (1981) 168-184
[19] Rahaman M., and De Jonghe L.C., Am. Ceram. Soc. Bull. 66 (1987) 782-785
[20] Wagner C.O., Passoja D.E., Hillery H.F., Kinisky T.G., Six H.A., Jansen W.T., and Taylor J.A., J. Vac. Sci. Technol. 21 (1982) 933-944
[21] Okumura H., Sakuma E., Lee J.H., Mukaida H., Misakawa S., Endo K., and Yoshida S., J. Appli. Phys. 61 (1987) 1134-36
[22] Lee E.H., Hembre D.M., Rao G.R., and Mansur L.K., Physical Review B, 48 (1993) 15540-15551
[23] Obraztova E.D., Nanophase materials (Kluwer Academ. Publishers, 1994) pp.483-492
[24] Wada N., Solin S.A., Wong J., and Prochazka S., J. Non-cryst. Solids 43 (1981) 7-15
[25] Serin V., Zanchi G., and Sévely, J. Microsc. Microanal. Microstruct. 3 (1992) 201-212
[26] Teo B.K., and Lee P.A., J. Am. Chem. Soc, 101 (1979) 2815-2832
[27] Marchand R., Laurent Y., and Lang J., Acta Cryst. B25 (1969) 2157-2160